

# MR of Hypoxic Encephalopathy in Children after Near Drowning: Correlation with Quantitative Proton MR Spectroscopy and Clinical Outcome

David J. Dubowitz, Stefan Bluml, Edgardo Arcinue, and Rosalind B. Dietrich

**BACKGROUND AND PURPOSE:** Quantitative MR spectroscopy has a proved role in the investigation of hypoxia caused by near drowning. To date, no studies have addressed the MR imaging changes that may also accompany this condition. The purpose of this study was to describe the MR imaging findings in children with hypoxic encephalopathy caused by near drowning and to compare these findings with the results of qualitative and quantitative proton MR spectroscopy and clinical outcome.

**METHODS:** Twenty-two children (6 months to 11 years old) admitted to the pediatric intensive care unit after near drowning incidents underwent cerebral MR imaging and quantitative proton MR spectroscopy. Clinical and imaging studies were reviewed retrospectively, and subjects were grouped according to outcome: good result, persistent vegetative state, and death. Images were scored for edema, basal ganglia changes, and cortical changes, and were compared with MR spectra and outcome at days 1 to 2, 3 to 4, and 5 or more.

**RESULTS:** Six patients had a good outcome, four remained in a persistent vegetative state, and 12 died. Generalized/occipital edema correlated with poor outcome. Indistinct lentiform nuclei margins on T1-weighted images were a frequent finding (78%). Basal ganglia T2 hyperintensity correlated with poor outcome, progressing from a patchy/peripheral distribution to diffuse high intensity. Patchy high T2 signal in the cortex or subcortical lines were specific but insensitive for poor outcome, as were brain stem infarcts.

**CONCLUSION:** MR images in children with hypoxic encephalopathy after near drowning show a spectrum of changes. The most sensitive prognostic result may be achieved by combining MR imaging with qualitative and quantitative MR spectroscopic data.

Interpretation of MR imaging studies in infants and children who have suffered hypoxic-ischemic insults may be difficult, as early findings are both subtle and complex. Nonetheless, in the evaluation of infants, MR imaging has proved to be extremely helpful in showing acute damage due to hypoxic encephalopathy (1-6) (Cohn MJ, Dietrich RB, Roth GM. Anoxic-ischemic events in infants: early MR findings. In:

*Annual Meeting of the American Society of Neuroradiology, Book of Abstracts, 1995:81*), although only anecdotal information is available regarding its use in evaluating similar damage in toddlers and older children (7-9). Near drowning is a common cause of hypoxic encephalopathy in this age group and is a useful model for all types of hypoxic encephalopathy. The term near drowning is used specifically to describe survival beyond 24 hours after cardiorespiratory arrest following submersion (10).

Of those who survive prolonged submersion, the majority have severe neurologic impairment, but as many as 30% may remain neurologically intact (11). Early in the clinical course it is necessary to distinguish between those who will die or be severely impaired and those who will have a good outcome, because the prognosis in profound hypoxic encephalopathy from any cause has significant impact on management within the intensive care unit, and also on determining future care.

Received August 5, 1997; accepted after revision May 29, 1998. D.J.D. is supported by travel grants from the Wellcome Trust and the Jameson Foundation of California.

Presented at the annual meeting of the American Society of Neuroradiology, Toronto, Canada, May 1997.

From the Huntington Medical Research Institutes, Pasadena, CA (D.J.D.); the Schulte Research Institute, Santa Barbara, CA (S.B.); the Huntington Memorial Hospital, Pasadena, CA (E.A.); and the University of California at Irvine, Orange, CA (R.B.D.).

Address reprint requests to Rosalind B. Dietrich MB, ChB, Department of Radiological Sciences, University of California at Irvine Medical Center, 101 The City Dr, Orange, CA 92668.

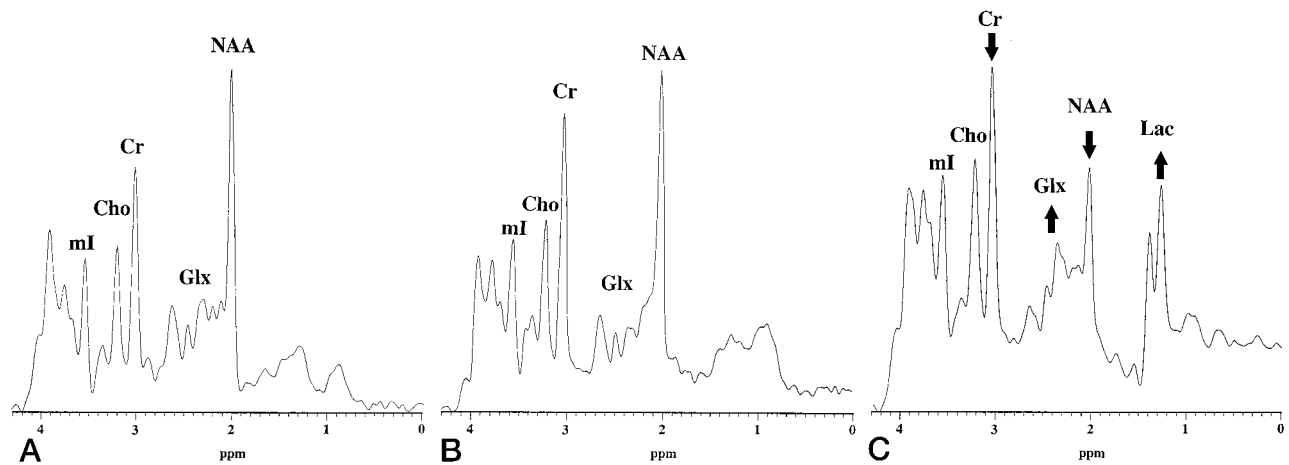
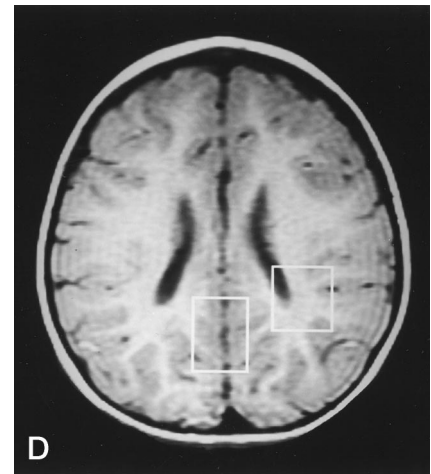


FIG 1. Typical MR spectra from occipital gray matter.

A–C, Gray matter spectra (1500/30, with a mixing time of 13.7) from a healthy 48-month-old boy (A); from a 40-month-old boy with good outcome, obtained on day 2 after submersion (B) (note small decrease of NAA/Cr; otherwise, the spectrum is normal); and from a 34-month-old boy who died, obtained on day 2 after submersion (C). In C, high concentrations of lactate are seen with the typical doublet at 1.3 ppm with 0.1 ppm separation. Glx is also elevated, and there is a reduction of Cr and a profound reduction of NAA, all indicating severe cerebral hypoxia. (mI indicates *myo*-inositol.)

D, The positions of the spectroscopic voxels are shown, indicating, at this level, the middle of the parietal white matter voxel and the top of the occipital gray matter voxel.



Quantitative proton MR spectroscopy allows quantitation of cerebral metabolites, which is useful in the evaluation of hypoxic encephalopathy in that it looks specifically for reduction in *N*-acetylaspartate (NAA) and creatine (Cr) and elevation in glutamine/glutamate (Glx) and lactate. Quantitative proton MR spectroscopy has a proved role in demonstrating abnormalities and in helping to predict final clinical outcome in this group of patients (12) (Fig 1); it is currently used in some clinical centers to aid in decisions related to termination of life support.

The aims of this study were to describe the range of MR imaging changes that may be seen after hypoxic encephalopathy due to near drowning and to investigate the significance of these changes by comparing our findings with the results of quantitative proton MR spectroscopy and clinical outcome. We also hoped to determine the usefulness and limitations of early MR imaging in predicting prognosis in these children.

## Methods

### Subjects

Our study group consisted of 22 consecutive children (6 months to 11 years old; mean age, 3.5 years) who were admitted to the pediatric intensive care unit between 1991 and 1997 after near drowning episodes resulting in cardiorespiratory

arrest and a Glasgow Coma Scale score of 3 through 7. Informed consent and approval of the Institutional Review Board were obtained in all cases.

### Imaging Techniques and Evaluation

Forty-seven combined cerebral MR imaging and quantitative proton MR spectroscopic studies were performed in the 22 children on a 1.5-T MR imager. All the children had initial MR studies performed 1 to 6 days (mean, 2.2 days) after submersion. Of these, 17 children had a second follow-up study performed 2 to 5 days (mean, 2.9 days) afterward, and six children had a third study performed 4 to 16 days (mean, 8.9 days) afterward. In addition, late follow-up studies were performed in two patients (2 and 3 months after the incident, respectively).

Axial spin-echo (SE) T1-weighted (600/11–20, repetition time/echo time [TR/TE]) sequences or gradient-echo (GRE) (250/11, with a 90° flip angle) and T2-weighted SE (3000/90–120) sequences or fast spin-echo (FSE) (2700–3700/98–112, with an echo train of 8) sequences were obtained. All images were reviewed retrospectively by two radiologists who were aware of the clinical history of near drowning but blinded to the MR spectroscopic findings and final clinical outcome. Images were scored for presence and distribution of edema, basal ganglia changes, cortical changes, and focal areas of hemorrhage and infarction. Edema was scored as focal (score = 1) if unilateral or if present in 50% or less of the cortex, as generalized (score = 2) if bilateral and present in more than 50% of the cortex, or as absent (score = 0). Basal ganglia margins were scored as normal (score = 0), as indistinct (score = 1), as swollen (score = 2), and as swollen and indistinct (score = 3). Basal ganglia signal was scored as normal (score = 0), as

TABLE 1: Distribution of findings of MR imaging/MR spectroscopic findings in patients in three outcome groups

Outcome Group	MR Findings				
	Edema	Fuzzy BG Margins	Abnormal BG Signal	Abnormal Cortical Signal	Abnormal MR Spectra
Good					
Case 1	No	Yes*	No	No	No
2	No	Yes*	No	No	No
3	No	No	No	No	No
4	No	Yes	No	No	No
5	No	Yes	No	No	No
6	No	Yes*	No	No	No
Vegetative State					
Case 7	Yes	Yes	Yes	Yes	Yes
8	Yes	No	Yes	Yes	Yes
9	Yes	Yes	Yes	Yes	Yes
10	Yes	Yes	Yes	Yes	Yes
Death					
Case 11	Yes	Yes	Yes	Yes	Yes
12	No	Yes	Yes	Yes	Yes
13	Yes	Yes	Yes	Yes	Yes
14	Yes	Yes	Yes	Yes	Yes
15	Yes	Yes	Yes	No	Yes
16	Yes	Yes	Yes	No	Yes
17	Yes	Yes	Yes	No	Yes
18	Yes	Yes	Yes	Yes	Yes
19	Yes	Yes	Yes	Yes	Yes
20	Yes	Yes	Yes	No	Yes
21	Yes	Yes	Yes	No	Yes
22	Yes	Yes	Yes	Yes	Yes

Note.—BG indicates basal ganglia.

\* Abnormal finding that reversed on subsequent examinations.

peripheral focal bright signal (score = 1), as patchy focal bright signal (score = 2), as diffuse high signal (score = 3), and as chronic signal changes (score = 4). The cortex was scored as normal (score = 0), as having focal bright signal (score = 1), as having subcortical lines (score = 2), as having both focal bright signal and subcortical lines (score = 3), and as showing atrophy (score = 4). Hemorrhage and infarction were scored as present or absent. MR imaging findings were considered abnormal in the presence of high T2 signal in the cortex or basal ganglia, brain stem infarction, or occipital or generalized edema. MR imaging findings were considered normal in the absence of these features.

Localized, quantitative, short-TE proton MR spectroscopy (1500/30, with a mixing time of 13.7) was performed in two standard locations: predominantly in the gray matter, in the posterior parietooccipital lobes (above the calcarine fissure across the midline); and in the white matter, in the deep parietal lobe (Fig 1D). These areas were chosen because they are known to be affected by hypoxia and because normative age-matched data were available for comparison. They were analyzed by examining peak ratios of the principal metabolites with respect to Cr and by assessing for presence or absence of lactate. Absolute quantitation was performed in 40 examinations using the method described by Kreis et al (13). In brief, the voxel was assumed to consist of brain water (extracellular and intracellular), CSF, and a component invisible to nuclear magnetic resonance (NMR). The proportions of brain water and CSF were calculated on the basis of their different T2 relaxation times. Seven single data points at TEs of 30, 40, 60, 90, 135, 270, and 1000 were constructed on a biexponential plot. An external reference was used to correct for coil loading, and the NMR-invisible component was assessed by the difference between the total signal (brain water and CSF) and a water phantom. The water content of brain can thus be calculated from the ratio of brain water to the combination of brain

water and NMR-invisible components. Data processing consisted of low-frequency filtering to remove residual water resonance and to produce a flat baseline. After zero-order phase correction of the spectra, the metabolite concentrations were calculated by integrating the peaks and curve fitting and by comparing them with calibrated phantoms. Postprocessing was done on a Sun-Sparc workstation using SA/GE software (GE Medical Systems, Milwaukee, WI). Comparison was made with data from age-matched control subjects who had been examined on the same scanner with the same imaging parameters. Standard graphs of metabolite levels versus age were constructed as described by Kreis et al (14). Normal values for any age could thus be read off a curve. For this study, spectra were considered abnormal if lactate was elevated or if NAA or Cr in gray matter was below 75% of that in healthy age-matched control subjects. Lactate was considered elevated if a clear doublet with 0.1 ppm separation was seen centered at 1.3 ppm. Because the findings in gray matter and white matter are similar in hypoxic insult (the gray matter changes being more sensitive and tending to precede those in white matter), we concentrated on the gray matter spectra for purposes of this article. In the four studies without absolute metabolite quantitation, the MR spectra were considered abnormal in the presence of lactate or if peak ratios of NAA/Cr in gray matter were below 75% of normal.

#### Clinical Outcome

The clinical data were reviewed and outcome was graded by cerebral performance category (CPC), as defined by Jennett et al (15) (Table 1). This was modified from the five-point scale into three clinically relevant groups, reflecting a final outcome of good (CPC, 1 to 2: good or moderate cerebral performance); persistent vegetative state (CPC, 3 to 4: severe cerebral disability or persistent vegetative state); or death (CPC, 5).

TABLE 2: Findings at MR spectroscopy versus outcome

Outcome	Metabolites*				
	Absolute NAA	Absolute Cr	NAA/Cr Ratio	$\beta\gamma$ -Glx	Lactate Present
Good (day 1-4)	n = 10 83 $\pm$ 6%	n = 10 90 $\pm$ 8%	n = 11 84 $\pm$ 7%	n = 10 105 $\pm$ 14%	n = 11 0
Vegetative state (day 1-16)	n = 9 62 $\pm$ 13%	n = 9 76 $\pm$ 5%	n = 11 65 $\pm$ 16%	n = 11 133 $\pm$ 21%	n = 11 6
Death (day 1-8)	n = 20 61 $\pm$ 16%	n = 20 72 $\pm$ 11%	n = 20 66 $\pm$ 19%	n = 20 138 $\pm$ 20%	n = 20 12

\* Lactate findings are expressed in terms of the number of patients in whom excess lactate was seen. Findings for other metabolites are expressed as a percentage of normative values from age-matched control subjects.

### Statistical Analysis

Imaging changes were correlated with clinical outcome and quantitative proton MR spectroscopic changes in the occipital gray matter. In addition, imaging and spectroscopic changes at different times after submersion (1 to 2 days, 3 to 4 days, and 5 days or more) were correlated with outcome to determine the prognostic strength of the MR imaging findings. Significance of differences among groups was tested by using one-way analysis of variance (ANOVA). Parametric data were assessed for strength of association by Pearson product-moment correlation coefficient. Nonparametric data were assessed by Spearman rank correlation coefficient and  $\chi^2$ -test (with continuity correction when the sample size was small) (SPSS for Windows, SPSS Inc, Chicago, IL).

### Results

Of the 22 patients, six had a good outcome, four were left in a persistent vegetative state, and 12 died. Forty-seven combined MR imaging and MR spectroscopic examinations were performed. High-quality MR images were obtained in 42 studies; in five studies, images were severely degraded or unavailable at the time of review. Forty-four MR spectroscopic studies were available for review, in which 40 had absolute quantitation of metabolites. Analysis of variance showed no significant differences in the distribution of age among the three outcome groups. The distribution of MR imaging and MR spectroscopic findings across the three outcome groups is summarized in Table 2.

#### MR Findings in Outcome Groups

**Good outcome.**—In the six children with good outcomes (11 studies obtained from 1 to 4 days after submersion and one late follow-up study at 2 months), the imaging findings were few. In no patient was there evidence of occipital or generalized edema or secondary findings of basal cistern or sulcal effacement.

Basal ganglia margins were abnormal and indistinct in five of six patients at the time of the initial study (mean, 2.3 days). Four patients had loss of the normal posteromedial margin (and/or posterolateral margin) of the lentiform nuclei. Subsequent imaging in three cases showed resolution in two and no change in one. One patient had swelling of the basal ganglia with retention of crisp margins at presentation (day 1). Subsequent imaging (day 2) showed normal-size basal

ganglia but loss of the normal margin, with complete return to normal by day 4. In no case was abnormal signal intensity seen on T1- or T2-weighted images. No cortical changes, hemorrhage, or infarction were seen in this group.

Absolute quantitation of principal metabolites was determined in 10 examinations. NAA was 79% to 93% of normal (mean, 83  $\pm$  6%), Cr was 79% to 104% of normal (mean, 90  $\pm$  8%), and NAA/Cr was 76% to 92% of normal (mean, 84  $\pm$  7%). In no examination was lactate present or Glx elevated (Fig 1B). No spectra were below the threshold for normality (as defined above). MR spectroscopic results are summarized in Table 2.

**Persistent vegetative state.**—All four patients (11 studies obtained between 1 and 16 days after submersion and one late follow-up at 3 months) had edema, which could be seen as early as 24 hours after submersion. Edema, which was initially focal, became generalized with time, and in one child compression of the basal cisterns developed. All children had signal intensity abnormalities of the basal ganglia with hyperintense areas on T2-weighted images (Fig 2). In addition, three had swelling of the basal ganglia and indistinct margins on T1-weighted images.

All four children had cortical abnormalities. In three, subcortical lines were seen on initial studies (days 1 to 2) and the fourth showed focal T2 hyperintensity (on day 12). The development of cerebral atrophy was also seen on intermediate studies (days 12 and 16) and at late follow-up (3 months) (Fig 2G and 2H). In addition, brain stem infarcts developed in two patients.

Absolute quantitation was determined in nine cases. NAA ranged from 36% to 75% of normal (mean, 62  $\pm$  13%) and Cr was 67% to 80% of normal (mean, 76  $\pm$  5%), with return to 92% at day 16 and to 99% at day 94. NAA/Cr was 38% to 90% of normal (mean, 65  $\pm$  16%). Lactate was present in six examinations as early as day 1. Glx was elevated initially (mean, 133  $\pm$  21%), but returned to normal levels after day 6 (Table 2). At the time of the first examination, three of four children had spectra below the threshold for normality. In the fourth child, the MR spectra did not meet the criteria for abnormality at presentation (day 1) but were appropriately abnormal



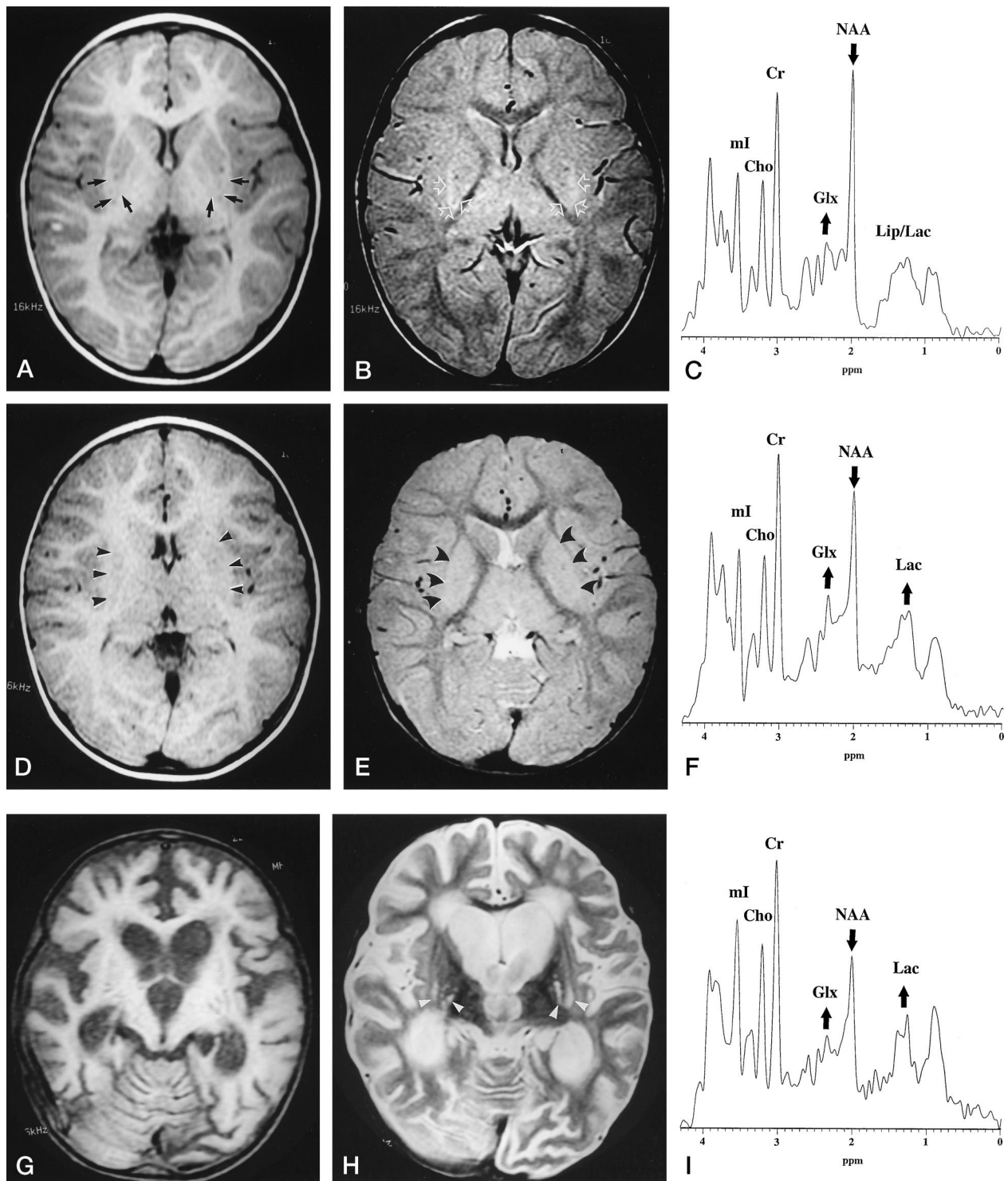


FIG 2. Progression of basal ganglia changes in a 19-month-old boy who remained in a permanent vegetative state.

A and B, Axial SE T1-weighted (600/20) (A) and proton density-weighted (3000/30) (B) MR images on day 1 show indistinct margins of lentiform nuclei (arrows, A) and high signal intensity peripherally (arrows, B).

C, Gray matter spectrum (1500/30, with a mixing time of 13.7) on day 1 shows reduced NAA and elevated Glx. The peak superimposed on the lipid and macromolecular resonances (Lip/Lac) may indicate excess lactate (a difficult diagnosis on this spectrum in isolation, but confirmed on the later examination at day 3).

D and E, Axial SE T1-weighted (600/20) and T2-weighted (3000/90) MR images on day 3. The lentiform nuclei are seen less clearly on the T1-weighted image (arrowheads, D) and have diffuse high signal intensity on the T2-weighted image (arrowheads, E).

F, Gray matter spectrum on day 3 shows considerably reduced NAA and elevated Glx and lactate.

G and H, Axial SE T1-weighted (600/20) (G) and T2-weighted (2500/90) (H) MR images at 3 months show diffuse atrophy and chronic changes in the basal ganglia with focal T2 high signal intensity changes in the posterior aspect of the lentiform nuclei bilateral (arrowheads, H).

I, Gray matter spectrum (1500/30, with a mixing time of 13.7) at 3 months shows almost absent NAA and elevated Glx and lactate.

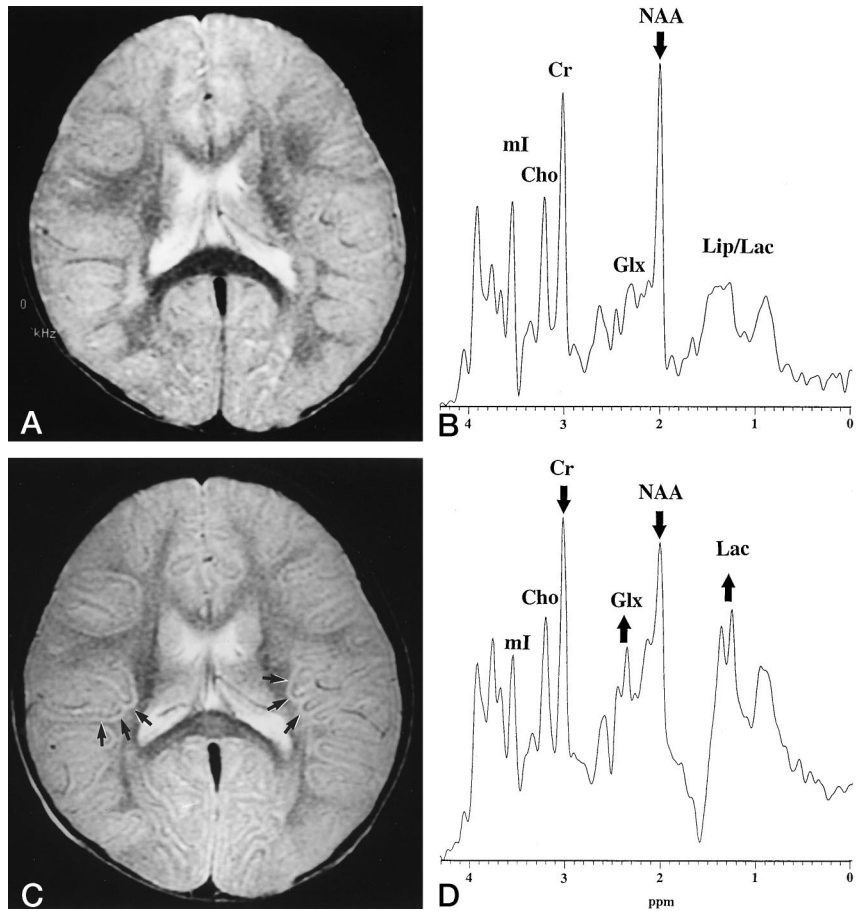
FIG 3. Development of subcortical "tram-tracks" in a 19-month-old girl who died.

A, T2-weighted SE image (3000/90) obtained on day 1 shows the presence of generalized edema.

B, Gray matter spectrum on day 1 shows reduced NAA. Elevated lactate cannot be readily defined on this early spectrum in isolation, but was confirmed on the later examination, at day 4.

C, T2-weighted SE image (3000/90) obtained on day 4 shows the development of extensive subcortical high signal intensity lines or "tram-tracks" (arrows).

D, Gray matter spectrum (1500/30, with a mixing time of 13.7) on day 4 shows considerably reduced NAA and Cr, and elevated Glx and lactate.



(NAA = 71%) by day 3 and remained abnormal on all subsequent examinations.

**Death.**—Of the 12 patients who died (20 studies obtained between 1 and 8 days after submersion), edema was seen in 11. At the first examination, edema was focal in the occipital cortex in five and generalized in five (Fig 3A). Delayed edema (day 5) developed in the occipital cortex in one patient, who also had abnormal basal ganglia but no edema initially. In three, edema was severe enough to cause compression of the basal cisterns. In all patients, indistinct margins of the basal ganglia were seen on T1-weighted images and hyperintensity was present on T2-weighted images by day 4. One patient with indistinct margins on T1-weighted images at day 2 had T1 hyperintense basal ganglia by day 4 (Fig 4). Basal ganglia swelling was also present in six of these patients, and cortical abnormalities were seen in four. In three children, subcortical lines developed (Fig 3C), and two showed focal high signal intensity on T2-weighted images (Fig 5A). One had evidence of laminar necrosis with high signal on T1-weighted images. Two patients also had brain stem infarcts (Fig 6).

Absolute quantitation of metabolites was determined in all examinations. NAA ranged from 41% to 103% of normal (mean,  $61 \pm 16\%$ ), and Cr ranged from 56% to 90% of normal (mean,  $72 \pm 11\%$ ). NAA/Cr was 47% to 93% of normal (mean,  $66 \pm$

19%). Lactate was present in 12 examinations as early as day 1. Glx was elevated in all early studies (mean,  $138 \pm 20\%$ ) (Table 2); in one case, returning to normal after 9 days. At the first examination, MR spectra were below the threshold for normal in 10 children; in the other two, the MR spectra were initially within normal limits (days 1 and 2, respectively) but were appropriately abnormal in both children by day 4 (NAA = 62%, Cr = 60%, moderate lactate; NAA = 63%, Cr = 64%, respectively) and all subsequent examinations remained abnormal.

#### Progression of Findings

The distribution of high signal in the basal ganglia progressed with time ( $P < .005$ ) (Fig 7). Initially, high signal intensity was seen peripherally along the lateral border of the putamen and the medial border of the globus pallidus on T2-weighted images (Fig 2B). After day 2 this pattern became more patchy (Fig 7). Beyond day 4, a diffuse high signal intensity pattern had developed in all patients (Fig 2E). No resolution of this finding was seen on subsequent imaging studies in any patient. On one late follow-up study the basal ganglia injury had evolved into the well-described chronic pattern of anoxic-ischemic injury with focal areas of gliosis in the posterior aspect of the lentiform nuclei and the ventrolateral thalamus (7,

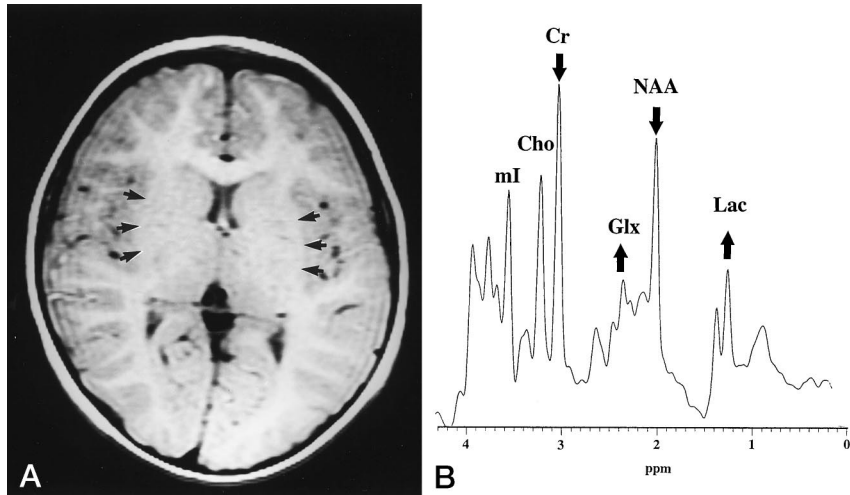


FIG 4. Development of T1 high signal intensity in the basal ganglia in a 1-year-old girl who died.

A, Axial T1-weighted SE image (800/11) shows indistinct basal ganglia margins on day 2 (arrows).

B, Gray matter spectrum on day 2 shows considerably reduced NAA and Cr, and elevated Glx and lactate.

C, High signal intensity is present in the basal ganglia on day 4 (arrowheads).

D, Gray matter spectrum (1500/30, with a mixing time of 13.7) on day 4 shows almost absent NAA, reduced Cr, and elevated Glx and lactate. Myo-inositol is also reduced (the significance of which is unclear).

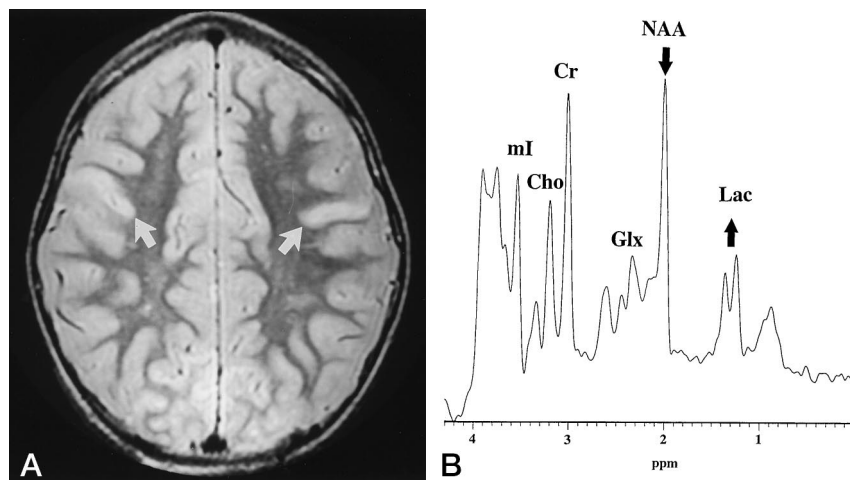
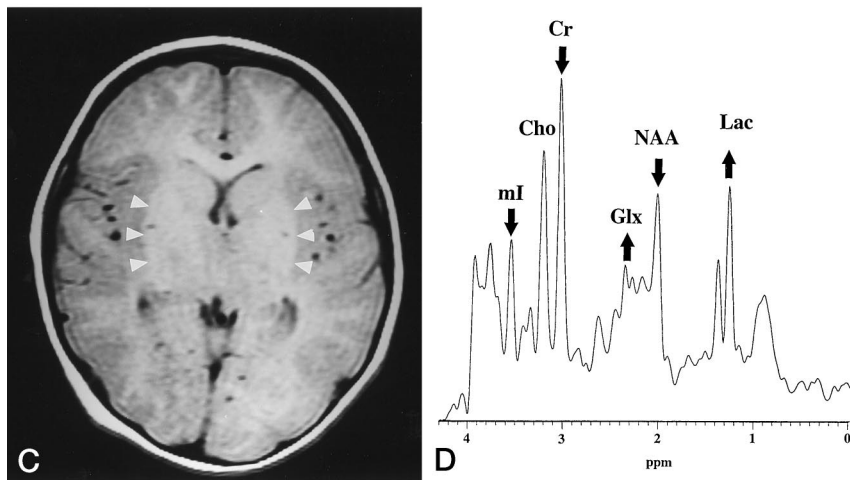


FIG 5. Focal high signal intensity in a 6-year-old boy who died.

A, Axial FSE T2-weighted image (3200/112eff, ETL = 8) obtained on day 1 shows focal areas of cortical hyperintensity (arrows).

B, Gray matter spectrum shows reduced NAA and elevated lactate.

16) (Cohn MJ et al, 1995) (Fig 2G and H). Edema also progressed with time ( $P < .05$ ); occipital edema was present as an early feature, whereas generalized edema was more prevalent beyond day 3. The presence of subcortical lines on T2-weighted images and its T1 correlate of an indistinct gray/white matter interface tended to be an early finding but failed to reach statistical significance.

### Correlation of MR Imaging Findings with Clinical Outcome

A strong correlation was observed between abnormal MR imaging findings (cortical or basal ganglia T2 signal changes or presence of occipital or generalized edema) and clinical outcome ( $P < .0001$ ). An examination of each of these findings independently revealed good correlation between the presence of oc-



FIG 6. Pontine infarction in a 2-year-old boy who died.

A, Axial FSE T2-weighted image (3200/112eff, ETL = 8) shows a high signal intensity infarction in the left pons (arrow).

B, Gray matter spectrum (1500/30, with a mixing time of 13.7) on day 2 shows markedly reduced NAA and probable excess of lactate. Elevated lactate cannot be readily defined on this early spectrum in isolation, but was confirmed on a later examination (not shown).

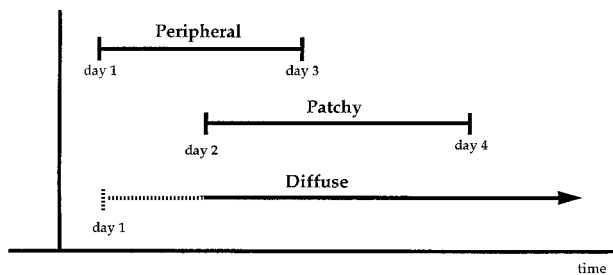
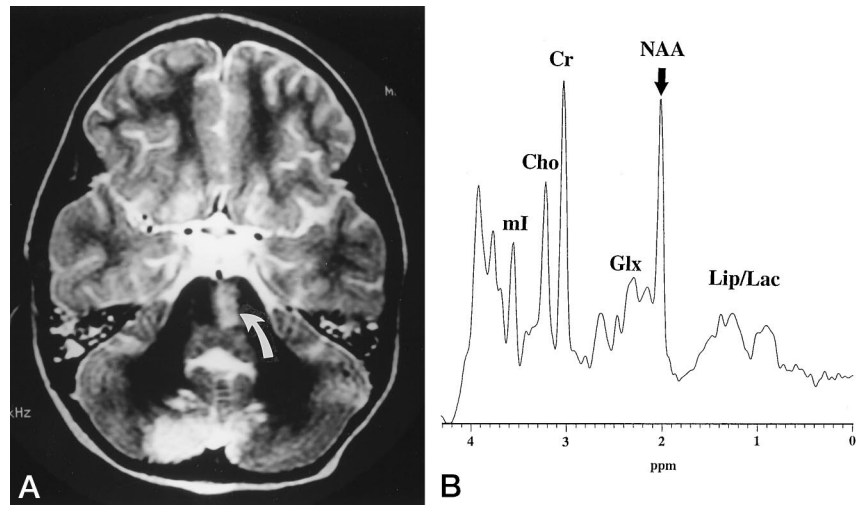


FIG 7. Time line of the distribution of basal ganglia T2 signal changes.

capital/generalized edema or of high signal in the basal ganglia on T2-weighted images and poor clinical outcome ( $P < .001$  for both findings). Abnormal signal intensity in the cortex on T2-weighted images was seen in 11 of 16 children who had a poor outcome (vegetative state or death) but was absent in another five children who had a poor outcome. While this finding lacks sensitivity (69%) it shows good specificity for a poor outcome (100%). The same was true of brain stem infarcts, which also were not sensitive for a poor outcome (25%) but showed good specificity (100%) when present. No reversibility of these findings was observed.

Indistinct basal ganglia margins on T1-weighted images was a common finding (78%) and an early and sensitive indicator that an anoxic-ischemic event had occurred. Correlation between this finding and clinical outcome, however, was poor. In three of the patients with a good outcome, the basal ganglia margins, although initially indistinct, regained their usual distinct margins on follow-up studies, suggesting reversibility of this sign in instances of mild hypoxia. In cases of severe hypoxia (vegetative state or death), the early T1 changes in the basal ganglia margins progressed to “invisible basal ganglia” (isointense with surrounding white matter) (Fig 4A), and in one instance, eventually became hyperintense (Fig 4C). In these cases of severe hypoxia, the corresponding T2-weighted images showed peripheral high signal intensity initially that progressed to diffuse high signal

TABLE 3: Findings at MR imaging versus outcome for the 1–2, 3–4, and  $\geq 5$ -day periods

MR Imaging*	Outcome			Total
	Good	Vegetative State	Death	
<b>1–2 days</b>				
Normal	5	1	1	7
Abnormal	0	3	9	12
Total ( $P < .005$ )	5	4	10	19
<b>3–4 days</b>				
Normal	5	0	0	5
Abnormal	0	3	6	9
Total ( $P < .001$ )	5	3	6	14
<b>5 or more days</b>				
Normal	1	0	0	1
Abnormal	0	4	4	8
Total ( $P < .025$ )	1	4	4	9

\* “Abnormal” was defined as the presence of high T2 signal in the cortex or basal ganglia, brain stem infarction, or occipital or generalized edema; findings were considered “normal” in the absence of these features.

intensity throughout the basal ganglia. In contrast to the T1 signal changes, the T2 changes, once established, did not reverse and correlated with poor outcome ( $P < .001$ ); these are, therefore, late and ominous signs.

To observe the impact of the timing of the examination on the MR imaging findings, and to establish the role of MR imaging in determining outcome, the results were further analyzed in smaller time frames for examinations on days 1 to 2, days 3 to 4, and day 5 or later (Table 3). For this analysis, abnormal MR findings were defined as presence of high T2 signal in



the cortex or basal ganglia, brain stem infarction, or occipital or generalized edema. Findings were considered normal in the absence of these features. Indistinct basal ganglia margins was a transient (and even reversible) sign, so this feature was less useful in determining outcome.

The best correlation with outcome was seen for MR imaging changes observed at days 3 to 4 ( $P < .001$ ). The positive predictive value of abnormal MR imaging findings at this time for a poor outcome (persistent vegetative state or death) was 100% (negative predictive value was also 100%). As early as days 1 to 2 there was still a good correlation between MR findings and outcome ( $P < .005$ ). The positive predictive value of abnormal MR findings at days 1 to 2 was also 100%. The negative predictive value was 71%, indicating the risk of a false-negative result at this early stage.

#### *Correlation of MR Imaging Findings with Results of MR Spectroscopy*

A strong correlation was observed between abnormal MR spectra (NAA, Cr, or NAA/Cr below 75% of normal or presence of lactate) and abnormal MR imaging findings (T2 signal changes in the basal ganglia or cortex, edema, or brain stem infarction) ( $P < .0001$ ). Examinations beyond 3 to 4 days showed perfect concordance between MR images and MR spectra and clinical outcome. Three early studies showed discordance, all false-negative MR spectroscopic studies obtained before 3 to 4 days. One study showed occipital edema and signal changes on T2-weighted images in the basal ganglia and cortex (day 1) (Fig 2A and B), the second showed generalized edema and signal changes on T2-weighted images in the basal ganglia and cortex (day 1) (Fig 5A), and the third showed focal occipital edema and patchy basal ganglia changes on T2-weighted images (day 2). The first remained vegetative, the other two subsequently died (early false-negative MR spectra). MR spectroscopic studies repeated in all cases were appropriately abnormal (on day 3 for the first child, on day 4 for the second and third children).

#### **Discussion**

Near drowning is a common cause of hypoxic encephalopathy in children; other causes include cardiocirculatory arrest, anesthesia accidents, and attempted strangulation. The mechanisms underlying the development of brain damage from all causes of hypoxic encephalopathy are extremely complex. As near drowning victims are usually neurologically intact before the event, they serve as excellent models for studying hypoxic encephalopathy. During a drowning episode, neurologic damage may be caused by a variety of factors, including cerebral hypoxia (following arrest of alveolar oxygen exchange), carbon dioxide narcosis, laryngospasm, pulmonary reflexes, or vagally mediated cardiac arrest (17). As cerebral hypoxia leads to circulatory arrest and de-

creased cerebral blood flow, the resulting neuropathologic changes reflect the effects of both hypoxia and ischemia. Changes occurring in arterial oxygen content, carbon dioxide content, pH, and blood pressure ultimately lead to brain injury, seen on MR images as edema, infarction, and hemorrhage (18).

Initially after the insult, compensatory responses come into operation to help protect the brain; temporarily, these lead to maintenance of regional cerebral blood flow (rCBF) owing to elevation of arterial blood pressure and redistribution of blood flow to vital organs. As the insult continues, the concomitant increase in carbon dioxide and decrease in blood pressure lead to a subsequent loss of autoregulation, reducing rCBF and resulting in decreased brain perfusion (18, 19). This results in infarction. The decrease in oxygen concentration leads to changes in capillary regulation and ultimately to capillary damage. When blood pressure is subsequently restored to normal values, resulting in reperfusion of previously injured tissue, hemorrhage may develop at the sites of previous capillary damage (18). In addition, the developing metabolic acidosis and hypoxemia rapidly alter the permeability of the blood-brain barrier, leading to vasogenic edema. Hemispheric swelling and brain herniation may occur in severe cases. The amount of edema is a reflection of the extent of the original and subsequent hypoxic effects.

By far the majority of patients who survive near drowning fall into two clinical groups, those who are normal after resuscitation (good outcome) and those who are vegetative (poor outcome). Vegetative patients ultimately die, but may remain in this state for extended periods of time. Although an accurate prediction of outcome based on clinical findings at presentation is extremely difficult (17–20), those patients who have absent muscle tone (Glasgow Coma Scale score of 3) and absent pupillary light reflexes are highly likely to die or to survive in a vegetative state (20). Ventilator-dependent patients in a coma represent a major dilemma early in their hospital course, as intensive care staff and parents together face decisions as to whether to disconnect life-support systems.

Both MR imaging and MR spectroscopy have better predictive value when examinations are performed beyond day 3. When studies are equivocal, it is helpful to repeat them 24 to 48 hours later in order to follow rising or falling trends in results. However, this time delay is not always practicable, as clinical decisions must frequently be made within a narrow window of time, in which care givers must balance the fact that life support needs to be continued at least until there is evidence of no hope of meaningful survival with the fact that decisions to terminate ventilatory support in the presence of cortical death must be made before breathing becomes autonomous (in order to prevent survival in a vegetative state). In this profound situation it is extremely helpful to have the results of MR studies to compare with clinical information. The early (and often subtle) irreversible MR imaging findings that we have described in this article

may be helpful in guiding management at this difficult stage.

As reported above, MR imaging findings include focal (particularly occipital) and generalized edema, basal ganglia changes, cortical abnormalities, and brain stem infarcts. There are important differences between the MR imaging findings seen in children with hypoxic encephalopathy and those described in infants (1–6) (Cohn MJ et al, 1995). Although focal and generalized edema are seen in both groups, the cortical changes and the observed progression of basal ganglia changes are different. In infants, the earliest basal ganglia changes are of diffuse T1 hyperintensity, which may be identified as early as day 1 after the hypoxic event. Later, the areas of hyperintensity become more focal and are positioned in a characteristic distribution involving the posterior lentiform nuclei and the ventrolateral thalamus. The appearance of the basal ganglia on T2-weighted images is initially normal and T2 changes are not identified until later, when either focal hyperintensity or hypointensity may be seen (Cohn MJ et al, 1995). By contrast, in the older children described in this study, the earliest basal ganglia signal intensity changes seen were on T2-weighted images. High signal intensity is present initially only along the periphery of the lentiform nuclei, gradually becoming more patchy and finally involving them diffusely. Although the T1 signal intensity of the basal ganglia is normal on early studies, the margins of the lentiform nuclei are frequently fuzzy or indistinct. The development of basal ganglia hemorrhage after near drowning has been described previously (8, 21), but it was not a frequent finding in our group of patients. Only in one child did the T1 signal intensity of the basal ganglia appear hyperintense, and this did not occur until day 4 (Fig 4). This T1 hyperintensity may have been due to the presence of early subacute hemorrhage or may have had an origin similar to the T1 high signal intensity seen in neonates.

It is likely that the basal ganglia T2 changes in older children reflect the presence of localized edema. Those seen in infants are more confusing; the T1 hyperintensity on early studies in infants may be due to the presence of hemorrhage, transient calcium, lipid from myelin breakdown products, free fatty acids or membrane lipids, or even from the paramagnetic effects of free radicals. The cortical changes seen are also different in the two groups, with laminar necrosis being common in infants and high signal intensity subcortical lines more frequent in the older children (8). It is possible that the high T2 signal intensity due to the higher water content of the white matter of the newborn brain obscures the presence of "tram-tracks" if present. Also, the softer consistency of the unmyelinated newborn brain may be more susceptible to necrosis, resulting in a higher prevalence of laminar necrosis in infants than in older children.

In both groups the characteristic distribution of injury is due to selective vulnerability of these areas of the brain during specific times of brain maturity.

These differences are probably related to the changing location of excitatory amino acid (glutamine) receptors and areas of myelination with age (19, 22, 23). At the time myelination occurs in a specific site, this site is extremely active metabolically and demanding of oxygen (19, 24), making it more vulnerable to periods of hypoxia.

The difference in the extent of early and final MR abnormalities may be an indication of partial reversibility of damage in certain parts of the basal ganglia but not in others. The concept of potential reversibility of anoxic-ischemic damage as reflected by reversibility of early MR imaging findings is a particularly exciting one as we approach the era of therapeutic intervention for the treatment of anoxic-ischemic injury. Apparent reversibility of early basal ganglia changes in infants with anoxic-ischemic encephalopathy has been described previously (Cohn et al, 1995), and this observation also appears to be true for the fuzzy basal ganglia sign seen in our subgroup of older children with a good ultimate outcome. Therefore, the presence of this subtle early imaging finding should alert physicians that a child needs to be closely monitored for the development of neurologic sequelae, but it does not in itself necessarily predict poor outcome. If early changes progress to basal ganglia T2 hyperintensity with or without cortical changes, then it is much more likely that the final clinical outcome will be poor.

As MR diffusion imaging and other new sequences with increasing sensitivity for demonstrating areas of brain disease become more widely available, we will undoubtedly see very early and subtle changes caused by anoxic-ischemic damage more often. These findings will perhaps afford us a better understanding of this complex problem (25). As yet, the relationship between early diffusion imaging findings and prognosis is unclear, and further study is needed. As we have shown, some findings may reverse (basal ganglia margins) and detection of similar abnormalities with more sensitive techniques may not necessarily imply poor prognosis.

In the first 24 to 48 hours, the presence of edema or T2 changes in the basal ganglia or cortex signal is both sensitive (100%) and specific (86%) for a poor outcome (persistent vegetative state or death). Even the presence of edema alone is helpful in predicting outcome, which supports similar findings from CT studies (21, 26, 27). Generalized edema or edema confined to the occipital cortex, on the other hand, did not reverse and was present in all patients in the vegetative outcome group and in 92% of those who died. As was previously found with MR spectroscopy (12), MR imaging findings could not differentiate patients who will die from those who will remain in a persistent vegetative state; however, since, clinically, the important distinction is between good and poor outcome, this is not a problem. The study was designed with this clinically important distinction in mind; thus, the reviewing radiologists were aware of the diagnosis of near drowning but were blinded to the clinical outcome and MR spectroscopic findings.

## Conclusion

In the evaluation of near drowning, MR imaging findings may be interpreted in isolation, but we found MR imaging and MR spectroscopy to be complementary. MR imaging and MR spectroscopy measure different parameters of hypoxia that are independent (but both correlate with poor outcome). The power of the combined examinations is superior to each individually (reducing potential false-negative results in early examinations). Because MR imaging and MR spectroscopy reflect different, but associated, parameters or factors in hypoxia, the MR spectroscopic study does not help to explain the pathophysiology of the MR imaging characteristics. The quantitative nature of MR spectroscopy makes it an extremely valuable tool when faced with the daunting task of making decisions with regard to termination of life support. In this situation, radiologists and spectroscopists are not asked to merely recognize hypoxic encephalopathy but also to play a pivotal role in determining prognosis and management. Intensive care physicians found the quantitative nature of MR spectroscopy extremely valuable both in making their own recommendations and in illustrating the degree of cerebral injury to the families of the patients. Nonquantitative MR spectroscopy also adds important information, although it may tend to underestimate a fall in NAA (as in hypoxic insult, Cr falls and is not a constant denominator in the NAA/Cr ratio). Such combined MR examinations should be considered for all these children, and MR spectroscopy may be performed as an integral part (6 minutes per sequence) of a routine brain MR examination. The availability of MR spectroscopy is, however, not as widespread as that of MR imaging, and thus such a combined study, although ideal, is possible only at a few centers. In most centers, in which MR spectroscopy is not available, the MR imaging features described above are sufficient to allow recognition of hypoxic encephalopathy, determination of prognosis, and planning of future management in these children.

## Acknowledgment

We acknowledge the help of Brian D. Ross throughout this study. We are also grateful to Toni Espinoza-Ferrel for help and advice with the statistical analysis, and to Dana Glidden for help with manuscript preparation.

## References

1. Barkovich AJ, Westmark KD, Partridge JC, Sola A, Ferriero D. **Perinatal asphyxia: MR findings in the first 10 days.** *AJNR Am J Neuroradiol* 1995;16:427-438
2. Westmark KD, Barkovich AJ, Sola A, Ferriero D, Partridge JC. **Patterns and implications of MR contrast enhancement in perinatal asphyxia: a preliminary report.** *AJNR Am J Neuroradiol* 1995;16:685-692

3. Baenziger O, Martin E, Steinlin M, et al. **Early pattern recognition in severe perinatal asphyxia: a prospective MRI study.** *Neuroradiology* 1993;35:437-442
4. Christophe C, Clerex A, Blum D, Hasaerts D, Segebarth C, Perlmutter N. **Early MR detection of cortical and subcortical hypoxic-ischemic encephalopathy in full-term infants.** *Pediatr Radiol* 1994;24:581-584
5. Rutherford MA, Pennock JM, Schwieso JE, Cowan FM, Dubowitz LMS. **Hypoxic ischaemic encephalopathy: early magnetic resonance imaging findings and their evolution.** *Neuropediatrics* 1995;26:183-191
6. Barkovich AJ, Sargant SK. **Profound asphyxia in the premature infant: imaging findings.** *AJNR Am J Neuroradiol* 1995;16:1837-1846
7. Barkovich AJ. **MR and CT evaluation of profound neonatal and infantile asphyxia.** *AJNR Am J Neuroradiol* 1992;13:959-972
8. Barkovich AJ. **Destructive brain disorders of childhood.** In: *Pediatric Neuroimaging*. 2nd ed. New York: Raven Press; 1995:107-175
9. Anderson ML, Wolpert SM, Kaye EM. **Vascular diseases and trauma.** In: Wolpert SM, Barnes PD eds. *MRI in Pediatric Neuro-radiology*. St Louis: Mosby-Year Book; 1992:177-204
10. Orłowski JP. **Drowning, near-drowning and ice-water submersions.** *Pediatr Clin North Am* 1997;34:75-91
11. Witte MK. **Near drowning.** In: Blummer JL, ed. *Practical Guide to Pediatric Intensive Care*. St Louis: Mosby; 1990:313-317
12. Kreis R, Arcinue E, Ernst T, Shonk T, Flores R, Ross BD. **Hypoxic encephalopathy after near-drowning studied by quantitative <sup>1</sup>H-magnetic resonance spectroscopy: metabolic changes and their prognostic value.** *J Clin Invest* 1996;97:1142-1154
13. Kreis R, Ernst T, Ross BD. **Absolute quantitation of water metabolites in the human brain, II: metabolite concentrations.** *J Magn Reson* 1993;102:9-19
14. Kreis R, Ernst T, Ross BD. **Development of the human brain: in vivo quantification of metabolite and water content with proton magnetic resonance spectroscopy.** *Magn Reson Med* 1993;30:424-437
15. Jennett B, Bond M. **Assessment of outcome after severe brain damage: a practical scale.** *Lancet* 1975;1:480-484
16. Dietrich RB, Kerrigan J, Chugani H, Gabriel R. **Cerebral palsy: correlation of MR imaging, history and clinical findings.** In: *Thirty-third Annual Meeting of the Society of Pediatric Radiology: Book of Abstracts*. Society of Pediatric Radiology; 1990:46
17. Levin DL, Morriss FC, Toro LO, Brink LW, Turner GR. **Drowning and near drowning.** *Pediatr Clin North Am* 1993;40:321-336
18. Volpe JJ. **Hypoxic-ischemic encephalopathy: biochemical and physiological aspects.** In: *Neurology of the Newborn*. 3rd ed. Philadelphia: Saunders; 1991:211-259
19. Hill A. **Current concepts of hypoxic-ischemic injury in the term newborn.** *Pediatr Neurol* 1991;7:317-325
20. Levy DE, Bates D, Coronna JJ, et al. **Prognosis in non-traumatic coma.** *Ann Int Med* 1981;94:293
21. Fitch SJ, Gerald B, Nagill HL, Tonkin ILD. **Central nervous system hypoxia in children due to near drowning.** *Radiology* 1995;156:647-650
22. Greenamyre JT, Penney JB, Young AB, et al. **Evidence for transient perinatal glutamatergic innervation of globus pallidum.** *J Neurosci* 1987;7:1022-1030
23. Barks JD, Silverstein FS, Sims K, et al. **Glutamate recognition sites in human fetal brain.** *Neurosci Lett* 1988;84:131-136
24. McArdle CB, Richardson CJ, Hayden CK, Nicholas DA, Amparo EG. **Abnormalities of the neonatal brain: MR imaging, II: hypoxic-ischemic brain injury.** *Radiology* 1987;163:395-403
25. Cowan FM, Pennock JM, Hanrahan JD, Manji KP, Edwards AD. **Early detection of cerebral infarction and hypoxic-ischemic encephalopathy in neonates using diffusion-weighted magnetic resonance imaging.** *Neuropediatrics* 1994;25:172-175
26. Murray RR, Kapila A, Blanco E, Kagan-Hallet KS. **Cerebral computed tomography in drowning victims.** *AJNR Am J Neuroradiol* 1984;5:177-179
27. Romano C, Brown T, Frewen TC. **Assessment of pediatric near-drowning victims: is there a role for cranial CT?** *Pediatr Radiol* 1993;23:261-265